

Chapter 2

Electrochemical Biosensors

2.1 Introduction

This book is about instrumentation with a strong focus on the electronics side of point of care devices. However, the mission of those electronics is to control and read electrochemical sensors accurately and reliably. Although those developing the electronics are neither expected nor required to be experts in Electrochemistry, it is highly desirable that they are familiar with at least some basic concepts governing electrode processes.

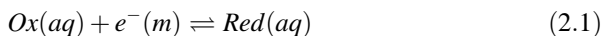
This chapter presents biosensors in the area of point of care but, to facilitate understanding, an overview of those basic aspects that influence electrode reactions and their study will be given first. Electrochemistry focuses mainly on interfacial phenomena, and relates chemical changes to electrical parameters, mainly current and potential.

Following an introduction of the main phenomena at play in an electrochemical process, some of the most common measurement techniques will be presented, distinguishing between direct and alternate current methods. Biosensors will be introduced next, highlighting what we believe are key design and performance considerations. The chapter ends with a section looking at the current trends in electrochemical biosensors for point of care applications.

2.2 Fundamentals of Electrochemistry

Electrochemistry is concerned with interfacial charge transfer processes, typically between a solid electrode and species in solution (Bard and Faulkner 2001). These charge transfer processes may involve electrons, as in the case in which both oxidized and reduced species remain in solution, or metal ions, as in the cases in which a metal is electrodeposited on or stripped off an electrode surface (Economou

and Kokkinos 2016; Herzog and Beni 2013; Lovrić 2010). In general, electrochemical processes are represented as reductions, as in the following equation, representing an oxidised species *Ox*, and a reduced species *Red*:



where (m) represents the metal electrode as source or sink of electrons. More specifically, it is the electrode Fermi level which exchanges the electrons with the species in solution. To facilitate the exchange, the electrode Fermi level may be adjusted externally through the application of a suitable voltage. When the Fermi level matches the energy of the frontier molecular orbitals of the *Ox/Red* species in solution, electrons can be exchanged. The energy level of the HOMO/LUMO¹ correlates with the formal potential, $E^{o'}$, of the *Ox/Red* pair, and the electrode potential, defined as the potential difference between the electrode and the solution, is described by the corresponding Nernst equation (Compton and Sanders 1996):

$$\phi_M - \phi_S = E^{o'} + \frac{RT}{F} \ln \frac{[Ox]}{[Red]} \quad (2.2)$$

ϕ_M and ϕ_S are the potentials of the metal and the solution, and the formal potential, $E^{o'}$, is a constant term that includes the contributions of the chemical potentials, activity coefficients, and any chemical equilibria affecting species *Ox* and *Red*. In the above equation, R is the gas constant ($8.314 \text{ J K}^{-1} \text{ mol}^{-1}$), T is the system absolute temperature (K), and F is the Faraday constant ($96,485 \text{ C mol}^{-1}$).

2.2.1 On the Measurement of Electrode Potentials

We have just seen the origin of electrode potentials, and how these depend on the concentrations of the species in solution involved in electron transfer processes. However, it is clearly not possible to measure the potential of a single electrode-solution interface, such as the one described above. Consequently, a second electrode is needed to close the circuit externally. This enables the measurement of a potential difference across *two* electrode-solution interfaces:

$$\Delta\phi = (\phi_{electrode\ 1} - \phi_S) - (\phi_{electrode\ 2} - \phi_S) = (\phi_{electrode\ 1} - \phi_{electrode\ 2}) \quad (2.3)$$

This difference of electrode potentials is the cell potential, and each electrode/solution interphase is considered a half-cell. If changes in the measured potentials are to be attributed only to changes at one of the electrode/solution interphases, then the composition of the second electrode—and hence its potential

¹HOMO: Highest Occupied Molecular Orbital; LUMO: Lowest Unoccupied Molecular Orbital.

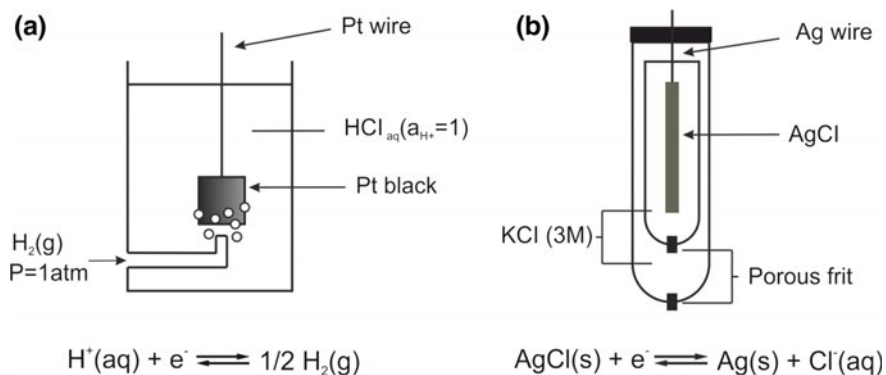


Fig. 2.1 Schematic representation of two different reference electrodes. **a** H^+/H_2 reference electrode. **b** Double junction Ag/AgCl reference electrode

—must remain constant during the experiment. Such electrodes of constant potential are reference electrodes, RE, and they usually comprise an electrode immersed in an electrolyte of known and constant composition, separated from the test solution by a permeable membrane, as represented in Fig. 2.1a. The importance of reference electrodes cannot be overstressed, as they are a critical part in any electrochemical experiment.

Thus, the simplest electrochemical cell is composed of two electrodes: a test or working electrode, and a reference electrode. However, two-electrode systems are only suitable for equilibrium measurements, and in dynamic electrochemistry experiments a third electrode needs to be introduced. Dynamic electrochemical experiments involve the departure from the system equilibrium position, bringing about the passage of current. The potential at the working electrode is measured against the reference electrode, through which no current flows. The working electrode is that at which the process under study takes place. Thus, the third electrode, also known as *auxiliary* or *counter* electrode, facilitates the passage of the current, closing the circuit. The potential of this auxiliary electrode normally neither known nor important, as the primary function of this electrode is to support the current passing through the working electrode.

2.2.2 On Notation

A simple shorthand notation is used to describe electrochemical systems. In this notation, accepted by the IUPAC, a slash to represents a phase boundary, a comma separates different species within the same phase, and a double slash represents a phase boundary of negligible contribution to the overall cell potential (i.e.: salt bridges) (Parsons 1974). The convention is that the reference electrode is written on the left-hand side and the test or working electrode on the right-hand side:

Reference electrode/solution//salt bridge//test solution/test electrode.

And the cell potential is calculated as

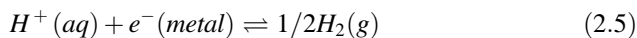
$$\Delta\phi = \phi_{\text{test electrode}} - \phi_{\text{reference electrode}} \quad (2.4)$$

2.2.3 Reference Electrodes

According to the IUPAC, “practical reference electrodes are (...) constructed so that their electrolyte solutions serve as salt bridges to the solutions under investigation. “Double” junction reference electrodes are recommended when the reference electrolyte contains ions that interfere with primary ion measurement or react with components of the test solution” (Buck and Lindner 1994). Thus, reference electrodes comprise both the metal electrode and the solution immediately in contact with it. In most cases, this solution is separated from the test solution by either a salt bridge or a membrane that protects the chemical composition of the interphase and thus preserves the electrode potential during an experiment. Double junction reference electrodes present two such salt bridges and are therefore the most stable and consequently generally preferred. Figure 2.1b represents a double junction reference electrode.

Two important reference electrode systems are the standard hydrogen electrode, SHE, and the silver-silver chloride electrode. The standard hydrogen electrode has been assigned a potential value of 0 V, and electrode potentials reported against it are referred to as standard potentials, E° .

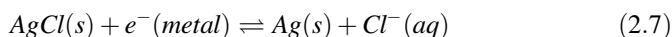
The standard hydrogen electrode consists of a platinized platinum (platinum black) electrode immersed in a solution with unit proton activity and over which hydrogen gas is bubbled to maintain a pressure of 1 atm. The potential determining equilibrium at this electrode is:



This is denoted as Pt/H₂(g) (P = 1 atm)/H⁺ (a = 1), and

$$(\phi_{RE} - \phi_S) = \Delta\phi + \frac{RT}{F} \ln \frac{a_{H^+}}{p_{H_2}^{1/2}} \quad (2.6)$$

The silver-silver chloride reference electrode is of special interest here because it forms the basis of most reference electrodes found in miniaturized devices. Its potential determining reaction is:



In turn, this is denoted as $\text{Ag}/\text{AgCl(s)}/\text{Cl}^-$, and

$$(\phi_{RE} - \phi_S) = \Delta\phi - \frac{RT}{F} \ln a_{\text{Cl}^-} \quad (2.8)$$

As this equation shows, the electrode potential is determined by the concentration of chloride ions in the solution. This is the reason why it is usually good practice to note the concentration of the chloride ion containing solution in contact with the Ag/AgCl electrode when reporting electrode potentials versus this electrode. If the concentration of chloride is unknown or cannot be controlled during the experiment, the Ag/AgCl electrode is referred to as a pseudo-reference electrode. Pseudo-reference electrodes are very common in miniaturized devices, where the fabrication of stable reference electrodes is impractical due to cost or to the difficulties in the integration of ionic membranes that can ensure a constant composition of the electrode-solution interphase throughout the measurement. One example of the successful microfabrication of a reference electrode relied on a thin hydrogel layer (ca. 1 μm) saturated with KCl photocured on a chlorinized silver micro-electrode. This device was used by Abbot's i-Stat system in the 1990s (Lauks 1990).

Whilst pseudo-reference electrodes are best avoided in potentiometric measurements for obvious reasons, they can and in fact are commonly used in three-electrode electrochemical measurements (see Sect. 2.3). Although it may be possible to ensure that their potential does not change significantly during the measurement, it is more difficult to know their potential value. In these cases, it may be convenient to add a small amount of an electroactive species of known formal potential, such as ferrocene, and thus report all measured potentials against it (Scholz 2010; Zoski 2007). Many excellent books and reviews address the subject of reference electrodes more rigorously (Inzelt et al. 2013; Scholz 2010), and the reader is encouraged to turn to them.

2.2.4 The Structure of the Electrode-Solution Interphase

The separation of charge at the electrode-solution interphase brings about the existence of electrode potentials. This charge separation results in a particular structure of the interphase, and different models have been proposed to describe it, as depicted in Fig. 2.2. The simplest of these models is the Helmholtz model, proposed as early as 1853 (Helmholtz 1853). In this model, the solution balances the charge at the electrode surface by means of a layer of ions of opposite charge distributed at a fixed distance from it. This distance, which is controlled by the hydration spheres of ions, is typically referred to as the Outer Helmholtz's plane. According to this model, the interphase may be described by a parallel plate capacitor:

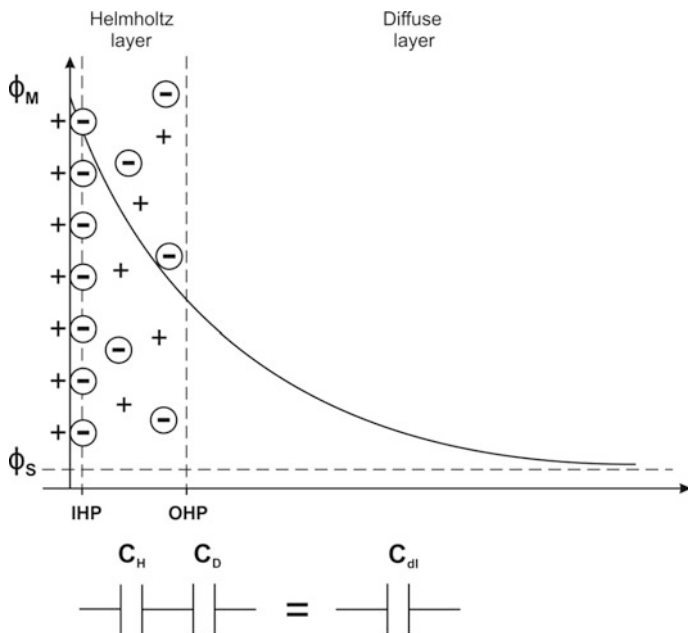


Fig. 2.2 Representation of the charge separation phenomena at the electrode-solution interphase, where the electrode surface is positively polarized

$$C_d = \frac{\epsilon \epsilon_0}{d} \quad (2.9)$$

where C_d is the interfacial capacitance, ϵ is the medium dielectric constant, ϵ_0 the permittivity of vacuum, and d is the distance between plates. However, this model does not account for the variations of C_d with potential, which are observed experimentally, and a more refined model is needed.

In 1910–1913, Gouy and Chapman independently proposed to account for the disorder in the solution side brought about by thermal motion of the ions (Chapman 1910; Gouy 1910a, b). In contrast to Helmholtz's model, which assumed the potential drop to be confined within a region as narrow as 1 nm from the electrode surface, Gouy-Chapman's theory assumes that the potential drop spreads into a slightly broader region inside of the solution. Thus, the highest charge density (ionic concentration) is found adjacent to the electrode and then progressively decrease into the solution bulk. The distance parameter in Eq. 2.9 may be thought of as an average distance, referred to as *diffuse layer*, which in this case depends on electrode potential and electrolyte concentration. The higher the electrolyte concentration, the smaller this region and the higher the capacitance observed.

A third model, devised by Stern (1924), combines the previous two, and assumes a structure in which a significant part of the charge is balanced by ions in close vicinity of the electrode, and the remainder by a diffuse layer spreading into the

solution bulk. This model overcomes the limitation of Gouy-Chapman's model, according to which the capacitance may increase almost unlimitedly at high electrolyte concentrations, as the model does not account for ionic size. Indeed, no ion can approach the electrode closer than its own radius. Thus, Stern's model proposes a plane of closest approach, referred to as Helmholtz's outer plane, OHP, and then a diffuse region. Thus, the interfacial capacitance may be regarded as the sum of two capacitances in series, corresponding to these two regions:

$$\frac{1}{C_{dl}} = \frac{1}{C_H} + \frac{1}{C_D} \quad (2.10)$$

where C_H is the capacitance of accruing from the charge at the OHP, and C_D is the capacitance arising from the charge distributed in the diffuse layer (Grahame 1947).

2.2.5 Electrode Kinetics

So far, we have only dealt with the case in which the electrode potential is determined by a chemical equilibrium of the species in solution in contact with it. Under these circumstances the net current observed is zero. However, by adjusting the energy level of the metal electrode, it is possible to affect the composition of the solution. This is known as dynamic electrochemistry, and is of great interest in electroanalysis (Albery 1975; Wang 2000).

A defining feature in electrochemistry is that the rate of electrode processes depends on electrode potential. Let us take the usual redox reaction:



the rate of this reaction may be written as

$$j = k_{red}[O]_0 - k_{ox}[R]_0 = \frac{i}{nFA} \quad (2.12)$$

where the rate constants for the reduction, k_{red} , and the oxidation, k_{ox} , processes are both potential dependent (Compton and Banks 2010). Here, n represents the number of electrons involved, F is Faraday's constant, and A the electrode area. Note that the subscript 0 next to the concentration terms means that we are referring to the concentration of O and R , respectively, *at the electrode surface*. Figure 2.3 shows a free energy diagram for the process, which has a potential-dependent energy barrier.

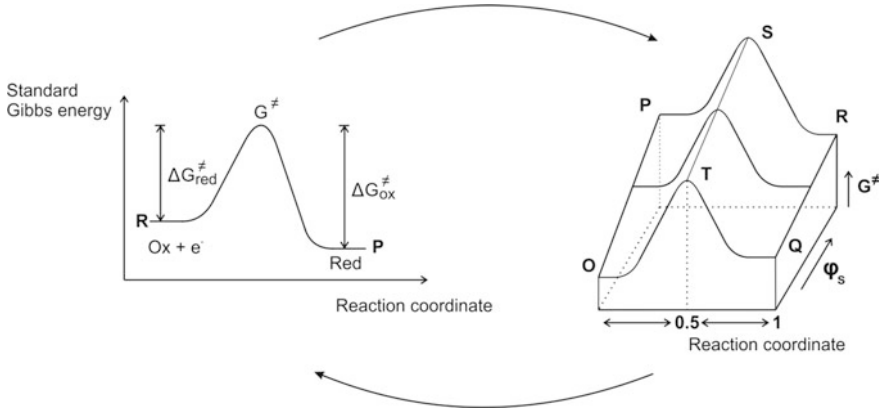


Fig. 2.3 Free energy diagrams representing an electrochemical process. The *right-hand picture* shows the process rate dependence with potential, while the *left-hand figure* represents the reaction energy diagram at a set potential

Thus, the rate constants depend on the free energy of activation, ΔG^\ddagger :

$$k_{red} = k_{red}^0 \exp\left(\frac{-\Delta G_{red}^\ddagger}{RT}\right) \quad (2.13)$$

and

$$k_{ox} = k_{ox}^0 \exp\left(\frac{-\Delta G_{ox}^\ddagger}{RT}\right) \quad (2.14)$$

Where the pre-exponential terms, k_{red}^0 and k_{ox}^0 are frequency factors describing the collisions of the reacting species (in solution) with the electrode surface. They are electrochemical rate constants, and their units stem from the fact that we have to relate a flux per unit area with concentrations, which have units of moles per volume. They are less than 10^5 cm s^{-1} (Scholz 2010).

The free energies of reactants (O and e^-) products (R), and that of the transition state can be expressed as:

$$G_{O+e^-} = \text{constant} + zF\phi_S - F\phi_M = (z-1)F\phi_S - F(\phi_M - \phi_S) \quad (2.15)$$

where z is the charge of the O species, and

$$G_R = \text{constant}' + (z-1)F\phi_S \quad (2.16)$$

The transition state can be expected to be somewhere in the way between the start and final states, and therefore:

$$G^\ddagger = \text{constant}'' + (z - 1)F\phi_S - \beta F(\phi_M - \phi_S) \quad (2.17)$$

where $0 < \beta < 1$. β is the charge transfer coefficient for the process (Guidelli et al. 2014), and it is typically assumed to be equal to $1/2$. This means that the transition state sits exactly mid-way between reagents and products (Pilling and Seakins 1995).

Now we can re-evaluate Eqs. 2.13 and 2.14, so that:

$$k_{red} = k_{red}^0 \exp\left(\frac{-(1 - \beta)F(\phi_M - \phi_S)}{RT}\right) \quad (2.18)$$

and

$$k_{ox} = k_{ox}^0 \exp\left(\frac{\beta F(\phi_M - \phi_S)}{RT}\right) \quad (2.19)$$

Thus, the rate Eq. 2.11 may be re-written as:

$$j = k_{red}^0 \exp\left(\frac{-(1 - \beta)F(\phi_M - \phi_S)}{RT}\right) [O]_0 - k_{ox}^0 \exp\left(\frac{\beta F(\phi_M - \phi_S)}{RT}\right) [R]_0 = \frac{i}{nFA} \quad (2.20)$$

We can safely assume that any change in the potential measured relative to the formal potential of the *Ox/Red* system, $E - E^0$, produces the same change in the magnitude $(\phi_M - \phi_S)$:

$$E - E^0 = (\phi_M - \phi_S) + \text{constant} \quad (2.21)$$

and the above equations may be re-written as a function of the measurable quantity $E - E^0$:

$$j = k_{red}^0 \exp\left(\frac{-(1 - \beta)F(E - E^0)}{RT}\right) [O]_0 - k_{ox}^0 \exp\left(\frac{\beta F(E - E^0)}{RT}\right) [R]_0 = \frac{i}{nFA} \quad (2.22)$$

when no net current flows, and $j = 0$, and there is no difference in the concentration between electrode surface and solution bulk values. If $\beta = 1/2$, then the Nernst equation is obtained:

$$\frac{[O]}{[R]} = \exp\left[\frac{F}{RT} (E - E^0)\right] \quad (2.23)$$

We have seen that the electrochemical rate constants are potential dependent but, it is important to stress that given the exponential nature of the dependency, a small change in applied potential has a huge effect on the process rate.

The Tafel equations are the result of assuming a sufficiently large overpotential, so that the net current flux is due only to either the reduction or oxidation process:

$$j_{red} = k_{red}^0 \exp\left(\frac{-(1 - \beta)F(E - E^0)}{RT}\right) [O]_0 = \frac{i_{red}}{nFA} \quad (2.24)$$

or

$$j_{ox} = k_{ox}^0 \exp\left(\frac{\beta F(E - E^0)}{RT}\right) [R]_0 = \frac{i_{ox}}{nFA} \quad (2.25)$$

Tafel plots, which enable the determination of the charge transfer coefficient, result from plotting $\ln|i|$ versus $(E - E^0)$, using current data from the region of electrode kinetics control.

Another important aspect of electrochemical processes is that the potential difference $(\phi_M - \phi_S)$ needs to be confined within a region suitable for electrons to tunnel between the electrode and the species in solution. This means that (i) dissolved species need to be able to approach the electrode to within 10–20 Å, and (ii) that the electrical double layer needs to be of a similar magnitude (Bard and Faulkner 2001; Henstridge et al. 2012). As it was described above, this may be achieved through the addition of sufficient concentration of supporting electrolyte. In weakly supported or totally unsupported media, the above equations need to be corrected (Albery 1975; Bard and Faulkner 2001).

Assuming that the right experimental conditions are given (well stirred solution so that the concentration of the electroactive species just outside the double layer is constant and equals that of the solution bulk), then the Tafel relation above predicts that the current would increase indefinitely with increasing potential. However, this is not observed experimentally because the concentration of electroactive species at the electrode surface is depleted and more needs to be supplied. This supply is achieved by mass transport, which will be covered in the next section.

2.2.6 Mass Transport Phenomena

Let us assume that electron transfer is sufficiently fast, and that any electroactive species reaching the electrode within electron tunnelling distance is oxidized or reduced. The rate of the electron exchange process is controlled by the rate of mass transport from the solution bulk to the electrode surface. Three mass transport phenomena participate in this exchange of material; these are diffusion, migration, and convection. Thus, the net flux of current exchanged can be broadly expressed as:

$$j_{\text{electron transfer}} = j_{\text{mass transport}} = j_{\text{diffusion}} + j_{\text{migration}} + j_{\text{convection}} \quad (2.26)$$

where

$$j_{\text{diffusion}} = -D\nabla C \quad (2.27)$$

$$j_{\text{migration}} = -\frac{zF}{RT}DC\nabla\phi \quad (2.28)$$

and

$$j_{\text{convection}} = Cv \quad (2.29)$$

where, for each species involved, C is its concentration, ∇C is the concentration gradient at the electrode surface, z is its charge, $\nabla\phi$ is the potential gradient, and v is the velocity of the liquid.

Equation 2.26 is more generally known as the Nernst-Planck mass transport equation (Cussler 2009; Levich 1962).

Diffusion involves a random, microscopic movement of species brought about by concentration gradients. The negative sign in Eq. 2.27 arises because the transfer of material occurs from high to low concentration regions. Diffusion is described mathematically by Fick's laws, of which Eq. 2.27 is known as Fick's first law. Fick's second law describes the changes in concentration of a species as a function of time:

$$\frac{\partial C}{\partial t} = D\nabla^2 C \quad (2.30)$$

These equations are extremely important in Electrochemistry, as the ultimate mode of approach of species to the electrode surface is always diffusion. As it will be shown below, solution of these equations with an adequate set of boundary conditions enables the electrochemist to predict and interpret experimentally observed currents.

Migration is another microscopic phenomenon, but this time it arises from the movement of charged species in an electric field, which, at the close vicinity of a polarized electrode, can be very significant. Electrochemical experiments are typically carried out in solutions containing an excess of an inert salt, referred to as supporting electrolyte, which mission is to carry the charge inside the solution, so that the contribution of the electroactive species, and hence this mass transport term, can be neglected. Typically, a 100-fold excess of supporting electrolyte ensures that the electroactive species under study do not transport charge through the solution, and hence the contribution of migration to mass transport can be neglected.

Convection, the third mode of mass transport, consists in the movement of macroscopic "packets" of solution. Convection may be natural or forced. Natural

convection arises from large density, temperature, or pressure gradients inside of the liquid, and is typically undesirable. Forced convection (Albery and Hitchman 1971; Compton et al. 1997; Cooper and Compton 1998; Levich 1962), on the other hand, can be a great aid as it provides an additional controllable variable to study reaction mechanisms or to improve the quality of the data recorded by electrochemical sensors. The most common ways to induce forced convection are channel cells (Cooper and Compton 1998; Snowden et al. 2010; Trojanowicz 2009), rotating electrodes (Albery and Hitchman 1971), power ultrasound (Banks and Compton 2003; Compton et al. 1997), and even electrode heating (Gründler et al. 1996; Zerihun and Gründler 1996). These methods allow the creation of a thin hydrodynamic layer over the electrode surface, of the order of a tens of microns, where the concentration gradient between the electrode surface and the solution is confined. By forcing a steady solution flow over the electrode surface, this concentration gradient remains constant over time, which leads to the observation of enhanced steady state currents at macroelectrodes.

2.2.7 A Word on Microelectrodes

Steady state currents may also be observed if the size of the electrode is smaller than that of the diffusion layer. This is what happens at micro- (Amatore 1995; Heinze 1993; Štulík et al. 2000; Zoski 2002) and nano-electrodes (Arrigan 2004; Clausmeyer and Schuhmann 2016; Godino et al. 2009). Due to their small size, microelectrodes present a number of advantages compared to macro-electrodes (Amatore 1995). First, they allow the measurement of a given solution without perturbing its composition. Bear in mind that, barring potentiometry, electrochemical requires the consumption of material at the electrodes, affecting composition locally. The extreme case is bulk electrolysis, used in electrosynthesis of new materials (Schäfer 2011), waste treatment (Fu and Wang 2011; Martínez-Huitle and Ferro 2006), or energy generation (Barbir 2013; Pistoia 2014; Scrosati and Garche 2010; Willner et al. 2009; Winter and Brodd 2004). This consumption is proportional to the passing current, which in turn is a function of electrode area. Thus, the composition changes caused by microelectrodes are nearly imperceptible. The passage of small currents has the additional advantage that microelectrodes, which currents are typically in the low nA range, are not exposed to ohmic drop losses to the same extent as macroelectrodes, which currents may be in the microampere range or higher.

Ohmic, or iR drop, stems from the solution resistance to the passage of current. Thus, the measured potential is given by:

$$E = (E_w - E_{ref}) + iR \quad (2.31)$$

In general, ohmic losses can be minimized by the introduction of a large amount of supporting electrolyte. Because the currents at microelectrodes are tiny, this term may be neglected even in the poorly supported or totally unsupported media (Bond 1994; Bond et al. 1984; Garreau and Savéant 1972; Limon-Petersen et al. 2009, 2010). Another beneficial consequence arising from microelectrodes is that the tiny currents passing through them often do not change the composition of the auxiliary electrode, allowing microelectrodes to be used in two-electrode systems without the need for a third, auxiliary electrode. A full discussion of the properties and behaviour of microelectrodes is well beyond the scope of this chapter, but a few hints will be given below. In addition, the following books and reviews may be of great use to the interested reader (Amatore 1995; Bond 1994; Heinze 1993; Schultze and Bressel 2001; Štulík et al. 2000; Zoski 2002).

2.3 An Overview of Electrochemical Methods: DC Versus AC Techniques

This section will focus on potential-controlled electroanalytical methods, including those based on direct and alternate current. These methods are based on the study of the current response obtained on application of different potential functions to the working electrode.

2.3.1 *Potential Step Technique*

This is one of the simplest electrochemical experiments and provides the basis for chrono-amperometric techniques. The experiment consists in the application of a potential jump from a value at which no current is observed, to another at which an oxidation or reduction process occurs, ideally at a mass transport-controlled rate. Figure 2.4 summarizes the main features of the potential step experiment. The concentration of the electroactive species at the electrode surface becomes zero, and the resulting transient current is a reflection of the instant concentration gradient. Under conditions of diffusion control, the current transient behaviour is described by the Cottrell equation:

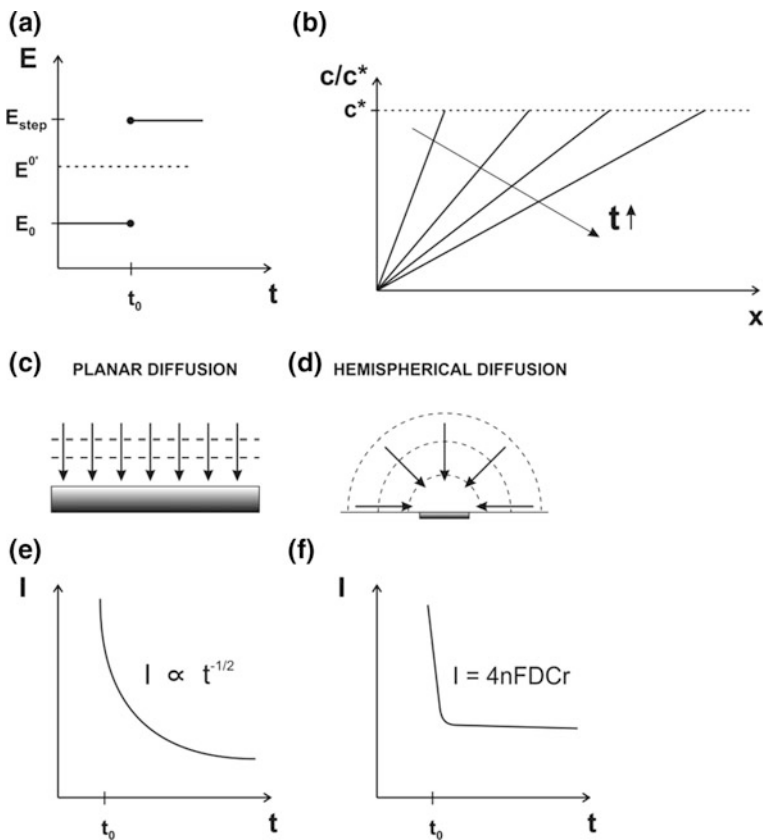


Fig. 2.4 **a** Plot of the potential step function. **b** Evolution of the concentration profiles with time. C^* represents the bulk concentration of the electroactive species. **c**, **d** Structure of the diffusion layer for two different diffusional regimes. **e**, **f** Typical transient currents for the case of planar diffusion (**e**) or hemispherical diffusion (**f**)

$$i(t) = nFAC\sqrt{\frac{D}{\pi t}} \quad (2.32)$$

This equation highlights the concentration dependence of the current, but, more importantly, the $t^{-1/2}$ time dependence which is the hallmark of planar diffusion (Compton and Banks 2010; Ngamchuea et al. 2014; Oldham 1979; Scholz 2010). Deviations from this equation occur both at very short times (up to tens of ms) and at times above 60 s. At very short times the current is greater than predicted by Cottrell's equation due to the charge/discharge of the double layer, which behaves as a capacitor. At longer times, the current deviates due to unwanted natural convection effects.

Microelectrodes, which due to their small size experience time independent currents at times $\tau > r^2/D$, pose a special case, and Cottrell's equation needs to be corrected. The following expression provides a very good approximation (Shoup and Szabo 1982):

$$i(t) = nFAC\sqrt{\frac{D}{\pi t}} + 4nFDCr \quad (2.33)$$

where r is the microelectrode radius in the case of disk microelectrodes (Scholz 2010).

Chronoamperometry may be used to determine diffusion coefficients, electrode geometry, or the concentration of electroactive species, and is the basis for amperometric measurements.

2.3.2 Cyclic Voltammetry

Cyclic voltammetry (Bard and Faulkner 2001; Compton and Banks 2010; Scholz 2010) is one of the most important electrochemical techniques. As shown in Fig. 2.5, it consists in the study of the current response following the application of a triangular potential wave at the working electrode.

As in the case of the potential step experiment, it is best to choose a starting potential at which no current flows. The potential is then swept up to a point where the sweep is reversed. Although normally the end potential and the start potential are the same, this is not necessary and depends on the specific needs of the study at hand. Assuming the presence of an electroactive species O , as the electrode potential approaches the reduction potential a current will begin to flow. This current will gradually increase until a maximum is reached at potentials past this reduction potential. The current then decays due to the rate limitation imposed by mass transport. At the beginning of the backward scan, reduction is still the main process until the potential approaches the formal reduction/oxidation potential of the electroactive species. If product R may be reduced reversibly, a current of the opposite sign appears. Current then increases until a new maximum is reached, again due to the effect of diffusion.

The shape of the cyclic voltammogram depends on the rates of electron transfer, mass transport, and any chemical steps coupled to the electroactive species. To discriminate between different phenomena, and to quantify these processes, the main experimental variable in this technique is the scan rate. Typical scan rates range between 1 mV s^{-1} up to a few V s^{-1} , although it is also possible to study very fast processes using microelectrodes and scan rates in the MV s^{-1} range (Amatore et al. 2000; Fortgang et al. 2010; Howell and Wightman 1984).

The relation of peak currents and position with scan-rate provides access to key mechanistic information with relative ease. For instance, the peak position of fully

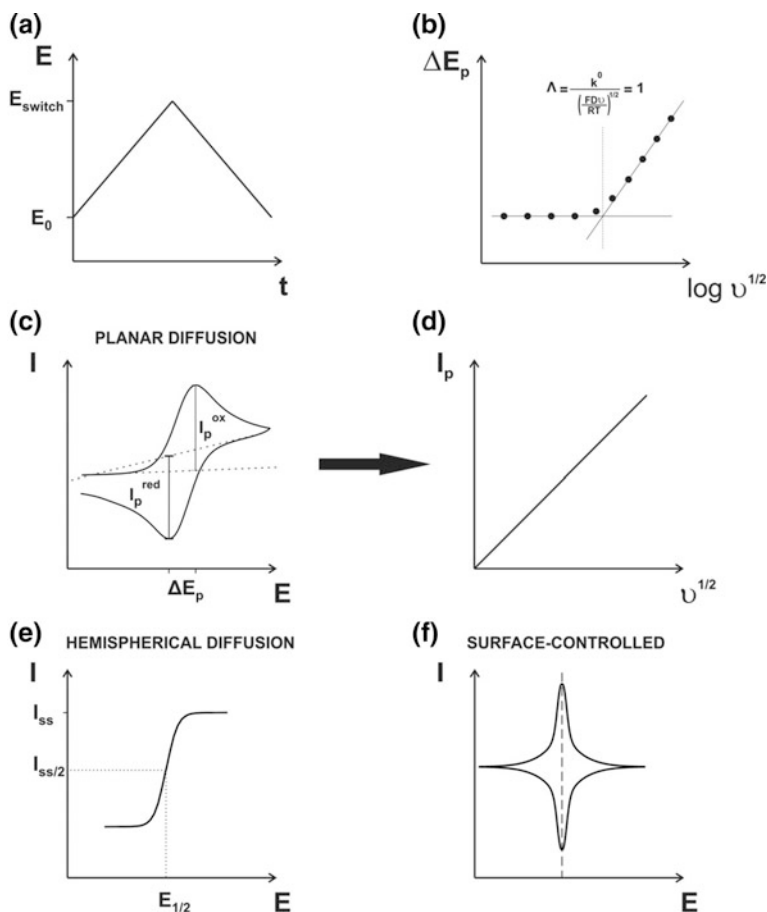


Fig. 2.5 **a** Representation of the triangular potential function used in cyclic voltammetry. **b** Plot of the peak-to-peak separation in the voltammograms against the logarithm of the square root of the scan rate. The intercept of the two linear zones is used to determine the heterogeneous electron transfer rate constant. **c** Typical cyclic voltammogram obtained under planar diffusion conditions. **d** Linear plot of the peak current intensity against the square root of the scan rate following the Randles-Sevcik equation. **e** Typical voltammogram for the case of a hemispherical diffusion regime. **f** Diagrammatic representation of a cyclic voltammogram obtained for the case of adsorbed species on the surface of the electrode

reversible (fast) electrochemical processes is independent of scan rate, and the separation between oxidation and reduction peaks is close to 59 mV. However, quasi-reversible and irreversible processes show peak potential shifts with increasing scan rate (Nicholson and Shain 1964), and the peak-to-peak separation increases with scan rate, as the kinetics of the electrode process become limiting. Plotting the peak-to-peak separation versus scan rate allows the determination of the electron transfer rate constant in quasi-reversible systems (Compton and Banks 2010).

Similarly, the magnitude of peak currents is also a tell-tale signal of electrode kinetics as well as of the presence of coupled chemical steps (Andrieux et al. 1978; Costentin et al. 2006; Savéant 2000, 2008).

The solution of the mass transport equations using boundary conditions corresponding to the application of a triangular potential wave leads to an analytical expression for the peak current. This expression is known as the Randles-Sevcik equation, and takes the following form:

$$I_p = \psi(\Lambda) nFAC \sqrt{\frac{nFD}{RT}} v \quad (2.34)$$

where $\psi(\Lambda)$ is a dimensionless current term that is a function of the electron transfer rate (Matsuda and Ayabe 1955). The term ranges from $0.3507 \leq \psi(\Lambda) \leq 0.4463$ for irreversible to fully reversible processes. Most experimental systems lay somewhere in between, and the value of this function may be determined using semi-empirical approximations based on the work of Nicholson and Shain (Nicholson 1965). These methods rely on the determination of the electron transfer rate constant, and their validity is usually restricted to cases where $\Delta E_p \leq 200$ mV. An alternative approach of wider validity for the determination of the electron transfer rate constant was proposed by Matsuda and Ayabe (1955). This method, summarized in Fig. 2.5b, is based on the determination of the scan rate at which the peak-to-peak separation begins to increase. At this scan rate, the dimensionless parameter $\Lambda = k_s / \sqrt{nFDv/RT} = 1$.

Voltammetric peak shifts are therefore of great diagnostic importance in cyclic voltammetry. In reversible systems, this is given by:

$$|E_p - E_{p/2}| = 2.218 \frac{RT}{nF} \quad (2.35)$$

whereas for (electrochemically) irreversible systems, the peak shift depends on the charge transfer coefficient, as:

$$|E_p - E_{p/2}| = 1.857 \frac{RT}{n\alpha F} \quad (2.36)$$

Cyclic voltammetry is very useful also in the study of chemical reactions coupled to electrochemical processes. In these cases, electron transfer reactions are indicated by a capital letter E, and any chemical steps are indicated by a capital letter C. Thus, for instance, a mechanism in which a chemical reaction follows an oxidation or reduction will be represented as an EC mechanism:



A key mechanism in biosensors is the EC' mechanism, where the C' represents a catalytic reaction in which the oxidised or reduced materials is turned back into its reduced or oxidised form to feed back into the E step, resulting in enhanced currents that are kinetically controlled by C' . A detailed account the most common cases and their analysis can be found in several books (Bard and Faulkner 2001; Compton and Banks 2010; Gosser 1993; Savéant 2008; Zoski 2007).

Although so far we have only dealt with cases involving species in solution, voltammetric techniques can also be applied to the study of surface-controlled processes. Some examples are those involving adsorption (Hulbert and Shain 1970), modified electrodes (Banks et al. 2003; Leddy et al. 1985; Lojou and Bianco 2004; March et al. 2015) which includes biosensors (Eggins 2002; Sadana and Sadana 2010; Turner 1987, 2013), and corrosion studies (Yebra et al. 2004).

The shape of voltammetric peaks for surface controlled processes differs very much from the mass transport-controlled case of species in solution. Peaks belonging to surface-controlled processes are sharper and the current drops much more abruptly after the peak as the electroactive species on the electrode is effectively consumed. Another difference is the separation between oxidation and reduction peaks which, in contrast to the case of species in solution, can be of 0 mV. Third, another important feature is the linear relation between scan-rate and peak current:

$$I_p = \frac{n^2 F^2 A \Gamma_0}{4RT} v \quad (2.39)$$

In this case, Γ_0 represents the surface concentration of the electroactive species.

2.3.3 Electrochemical Impedance Spectroscopy (EIS)

In contrast to potentiometric and voltamperometric techniques, which are direct current methods, electrochemical impedance spectroscopy involves the study of the current-potential response following application of alternate signals, usually of sinusoidal nature (Barsoukov and Macdonald 2005; Gabrielli 1995; Orazem and Tribollet 2011).

$$E(t) = E_{polarization} + \Delta E \sin(\omega t) \quad (2.40)$$

where $E_{polarization}$ is the base working electrode potential, ΔE is the potential perturbation amplitude of the sine wave, and ω is the signal frequency in rad s^{-1} . The response of linear systems is a sinusoidal current of the same frequency, but different amplitude and phase:

$$I(t) = \Delta I \sin(\omega t + \phi) \quad (2.41)$$

where ΔI is the current amplitude and ϕ is the phase-shift angle.

The impedance, Z , is defined as the ratio between potential and current:

$$Z = \frac{E(t)}{I(t)} = \frac{\Delta E \sin(\omega t)}{\Delta I \sin(\omega t + \phi)} \quad (2.42)$$

If both $E(t)$ and $I(t)$ are in phase and $\phi = 0$, then Eq. 2.42 is simply Ohm's law. However, Electrochemical systems are highly non-linear and present both real and imaginary components (Gabrielli 1995).

The performance of EIS relies on the use of frequency response analyzers, which allow the study of the potential-current response of a system at different frequencies, typically ranging from a few mHz up to 1 MHz. As we have seen, electrochemical impedance spectroscopy studies the impedance response of electrochemical systems to small amplitude perturbations. The most common case is the study of the frequency response following the application of a small potential signal. The experimentalist should strive to work under linear response conditions. Electrochemical systems can be highly non-linear due to mass transport and coupled chemical kinetics, and linearity is controlled by the choice of polarization potential and perturbation amplitude. The use of very small perturbations (1–10 mV) almost always ensures that the linearity assumption is met, but they may result in problems caused by electrical noise. Thus, quoting Orazem and Tribollet, *“the correct amplitude represents a compromise between the desire to minimize nonlinear response (by using a small amplitude) and the desire to minimize noise in the impedance response (by using a large amplitude)”* (Orazem and Tribollet 2011). For instance, an adequate amplitude range for the study of faradaic phenomena may be 5–20 mV, whereas amplitudes of 50 mV or greater may be used in the study of non-faradaic systems. However, the best conditions will depend not only on the electrochemical system, but also on the instrumentation used (the faster the potentiostat the better) and the experimental set-up (i.e. use short, shielded cables to avoid parasitic impedance, particularly at high frequencies, and work in a Faraday cage to avoid electrical noise).

Figure 2.6 shows the most common representations for impedance spectra. These are known as Bode and Nyquist plots. Bode plots present the impedance magnitude and phase shift as a function of frequency, usually on a logarithmic scale to facilitate the observation of different events across the whole spectrum. Bode plots can be used to identify and analyze faradaic and non-faradaic phenomena. In Nyquist plots, on the other hand, the imaginary part of the impedance is plotted against the real part. It is important that both axes display the same scale to facilitate the analysis. Nyquist plots are not subject to the scale compression effect of the logarithmic bode plots, and thus low frequency phenomena can be easily appreciated, which makes Nyquist plots greatly useful in the study of faradaic phenomena.

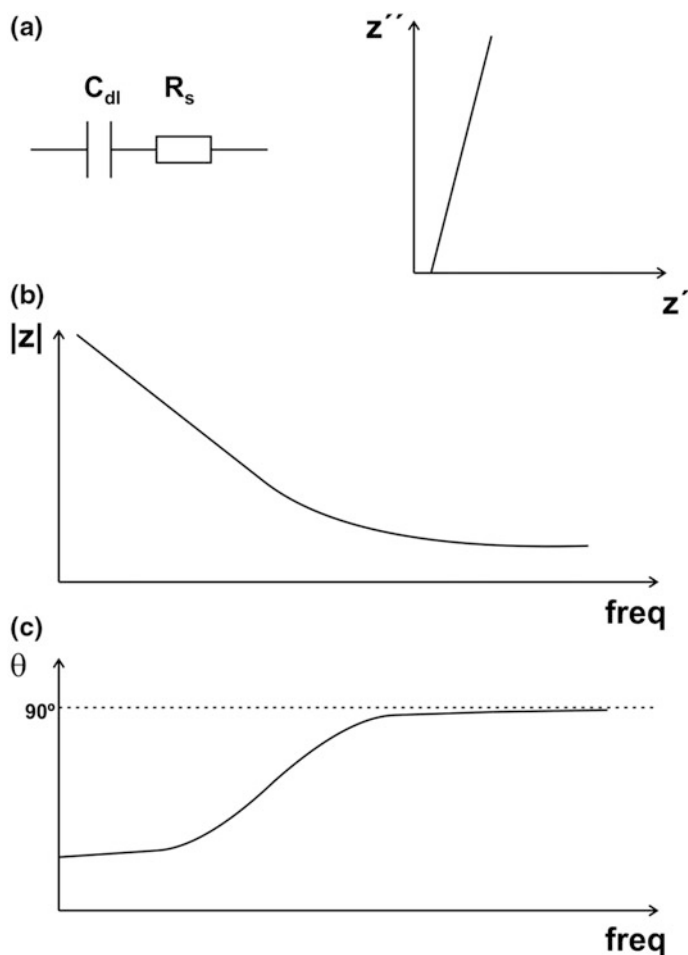


Fig. 2.6 **a** Equivalent circuit for an electrochemical cell in the absence of faradaic processes (*left*), and corresponding Nyquist plot (*right*). **b** Bode plot for circuit (**a**) representing the magnitude of impedance versus frequency and, **c** Bode plot representing the phase shift angle for the same system versus frequency

The most common way to analyse electrochemical impedance data is by means of so-called equivalent circuits (Orazem and Tribollet 2011). This approach consists on the assimilation of electrochemical phenomena (interfacial charging, electron transfer, and mass transport) to electrical elements and arranged in an equivalent circuit that matches the structure of the electrochemical cell. Figure 2.7 presents the Randles circuit and the correspondence of its elements to a typical electrochemical cell.

In general, the electrode-solution interface is represented by a capacitor, and the solution between electrodes as a resistance. Faradaic processes, characterized by

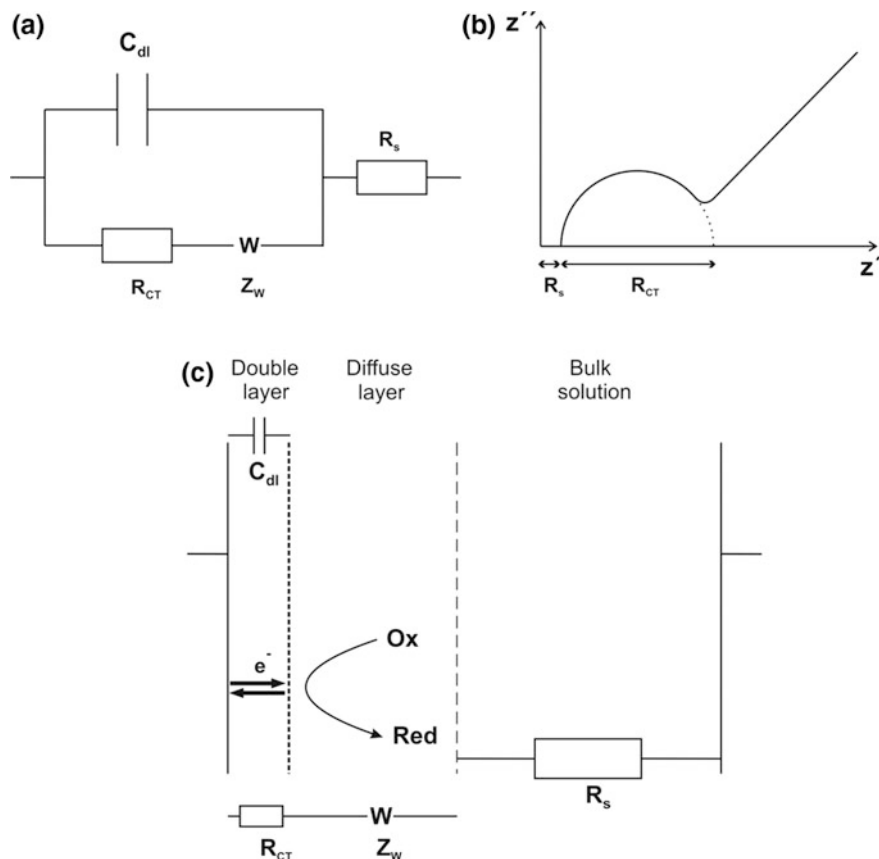


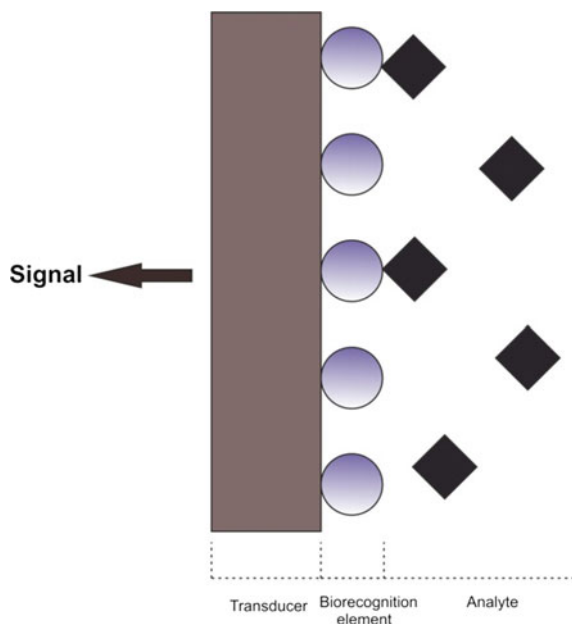
Fig. 2.7 a Randles circuit and its corresponding Nyquist plot (b). c Presents the correspondence between the different circuit elements and the different physico-chemical processes involved in the electrode process

charge transfer at the electrode-solution interphase, are represented by a resistance in series with the interfacial capacitance. The contribution of mass transport is represented by a Warburg element (Gabrielli 1995) connected in series to the charge transfer resistance.

2.4 Electrochemical Biosensors: Design, Construction and Performance

Broadly speaking, biosensors are a special type of chemical sensor where the recognition element coupled to the transducer is of biological origin (Eggins 2002; Yebra et al. 2004). A more thorough definition can be found in (Biosensors and

Fig. 2.8 Diagrammatic representation of the different components integrating a biosensor



Bioelectronics 2017), and as the interested readers will find, the kinds of biological recognition elements is considerably long and includes even “biomimetic”, or artificial, receptors.

The first reported biosensor was a glucose biosensor based on a membrane containing glucose oxidase coupled to a Clark oxygen electrode (Updike and Hicks 1967).

Figure 2.8 provides a summary of the key design aspects around biosensors, which are generally classified according to biorecognition element type and transduction method. In terms of biological recognition elements, enzymes and antibodies are the most common ones, although biosensors based on DNA fragments and on artificial receptors are also important. As far as transduction methods are concerned, most biosensors are either photometric or amperometric, but other methods based on fluorescence (Benito-Peña et al. 2016; Goedhart et al. 2014), surface plasmon resonance (Olaru et al. 2015), quartz crystal microbalance (Cooper and Singleton 2007; Minunni et al. 1995), and impedance measurements (Katz and Willner 2003) are also used in biosensing.

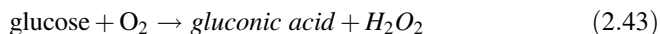
This section aims to give an overview of the main biosensor types, focusing on performance and suitability aspects.

2.4.1 Enzymatic Biosensors

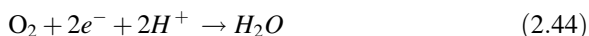
Enzymatic biosensors rely on the enzymatic reaction of the analyte with a particular enzyme, and on the monitoring of either the enzyme activity, or the quantification of a product of the enzymatic reaction at a given end-point (Habermüller et al. 2000).

Enzymes are highly specific molecular machines able to catalyse the conversion a substrate (the analyte) into a product (Cornish-Bowden 2011). Enzymes may be coupled to transducers in a number of different ways, but typically they are incorporated inside membranes that help stabilize them and control the access of the analyte of interest (Eggins 2002; Mulchandani and Rogers 1998; Ronkainen et al. 2010; Sadana and Sadana 2010).

The first glucose biosensors worked by measuring the rate of oxygen consumption of the enzyme glucose oxidase in the presence of glucose (Updike and Hicks 1967). The enzyme glucose oxidase turns glucose into gluconic acid, using oxygen as electron receptor, according to the following reaction:



the electrode process (-0.7 V vs. Ag) in this biosensor was:



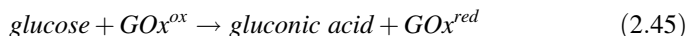
Subsequent glucose biosensors (Karyakin et al. 1995; Wang 2008) relied on the quantification of the hydrogen peroxide produced in the enzymatic reaction. These devices marked a *first generation* of glucose biosensors. These biosensors suffered from two main kinds of issues. First, they depended on oxygen as the electron acceptor and, second, their high polarization potentials exposed them to interferences from other electroactive species typically present in physiological samples, such as ascorbic or uric acid.

The introduction of so called redox mediators to substitute oxygen as the electron acceptor limitation partially solved these problems, marking the appearance of so-called *second generation* biosensors (Heller 1990; Scheller et al. 1991). These redox mediators acted as electron shuttles between the enzyme and the electrode, and facilitated the monitoring of enzyme activity which depends on the substrate concentration. In order to work, these mediators need to present a number of important properties:

- (i) they need to be able to react reversibly with the enzyme.
- (ii) they must display fast electrode kinetics.
- (iii) they need to be pH-independent.
- (iv) the formal potential of the redox mediators should be low to prevent interferences from other electroactive species present in the sample, including oxygen.

- (v) they should be stable both in their oxidized and reduced states.
- (vi) they should be non-toxic.

The operation of second generation glucose biosensors is described by the following mechanism:



Most present-day biosensors are of this type, although differences may be found in the choice of mediator, enzyme, and biosensor-solution interface.

Last, *third generation* biosensors are those in which electrons are directly exchanged between the enzyme and the electrode (Gorton et al. 1999; Varfolomeev et al. 1996; Zhang and Li 2004). This type of biosensors is rather exceptional because in most cases electron transfer between the electrode and the enzyme active site is hindered by the enzyme protein shell. As it was discussed above, effective electron transfer requires distances of the order of a few nm at most between the electrode and the redox centres. In most enzymes, including glucose oxidase, the active site is deeply buried in the enzyme structure, which makes direct electron transfer with an electrode very hard. Although this situation is gradually being turned by nanomaterials (Taurino et al. 2016; Vashist and Luong 2015; Wu et al. 2014; Yarman et al. 2011; Zhang and Li 2004), the existing examples of third generation biosensors are still relatively few, and mostly based on small enzymes such as cytochrome c and peroxidases (Stoica et al. 2006; Xu et al. 2014; Yarman et al. 2011).

2.4.2 Enzyme Kinetics

Most biosensors rely on enzymes, whether as main biorecognition elements in enzymatic biosensors, or as labels in affinity-based biosensors. Biosensors monitor the activity of these enzymes through measurements of concentration changes in either a substrate or a product of the enzymatic reaction. Enzyme kinetics are described by the so-called Michaelis-Menten equation (Cornish-Bowden 2011), which describes the rate of enzymatic reaction as a function of substrate concentration:

$$v = \frac{k_{cat}e_0a}{K_m + a} \quad (2.48)$$

where k_{cat} represents the enzyme-substrate dissociation rate constant, e_0 is the initial enzyme concentration, a is the substrate concentration, and K_m the Michaelis constant. K_m corresponds to the substrate concentration for which the velocity of the reaction is a half of the maximum velocity.

This equation may be derived using the steady-state approximation on the enzyme-substrate complex (Pilling and Seakins 1995) from the following mechanism:



where E represents the enzyme, A is the enzyme substrate, EA represents the enzyme-substrate complex, and P the resulting product of the enzymatic reaction.

In addition,

$$K_m = (k_{-1} + k_{cat})/k_1 \quad (2.52)$$

k_{cat} is also known as the enzyme turnover number, and its reciprocal gives the number of cycles that the enzyme may undergo per unit time. This brings us to the meaning of the activity units that are typically given instead of enzyme concentration. The relevant figure of merit in enzymes is not their concentration, which is often unavailable. Instead, it is more convenient to report on their activity. Activity units, symbolized as IU (international unit), are defined as the amount of enzyme that can turn 1 μmol of substrate in 1 min under a set of given conditions (Cornish-Bowden 2011). Stating the conditions under which an activity has been determined is important, because enzymes are extremely sensitive to changes in ionic strength, pH or temperature, to name three of the variables that are typically controlled in biosensing. Enzyme activity may also be inhibited by the presence of certain substances. This forms the basis for the development of many toxicity biosensors. One common example is the detection of heavy metals using acetylcholinesterase (Amine et al. 2006).

Also, too high substrate concentrations may also inhibit the activity of certain enzymes. An important case is that of horseradish peroxidase, HRP, one of the most commonly used enzymes in biosensing. Horseradish peroxidase catalyses the reduction of hydrogen peroxide, and is commonly used in enzyme cascades in combination with oxidases (Arya et al. 2008; Azevedo et al. 2005; Garjonyte et al. 2001; Gorton et al. 1992; Singh et al. 2006; Sirkar et al. 2000; Vijayakumar et al. 1996), but also to label antibodies in immunosensing (Burcu Bahadir and Kemal Sezginürk 2015; Chikkaveeraiah et al. 2012; Laocharoensuk 2016; Lim and Ahmed 2016; Rama and Costa-García 2016; Wan et al. 2013). When the concentration of H_2O_2 exceeds a certain threshold (in the low mM range), the activity

of peroxidases is inhibited, and the enzyme may even denature, leading to lower than expected signals (Dequaire et al. 2002).

2.4.3 *Immunosensors*

Immunosensors are a type of affinity biosensor that use antibodies to recognize the presence of a target antigen (Yakovleva and Emneus 2008). In contrast to enzymatic biosensors, which can work continuously as long as their substrate is present, the stability of the antigen-antibody complex makes immunosensors unsuitable for continuous measurements. Immunosensors are normally single-use devices because, once the antibodies on the biosensor have reacted with the antigen present in a sample, they cannot be used again unless this antigen-antibody complex is broken. On the other hand, immunosensors are much more sensitive than enzymatic biosensors, and turn out ideal for the detection of small molecules, proteins, or even whole cells at ppb level or lower.

There are different ways to exploit antigen-antibody interactions in biosensors, many of them based on their ELISA counterparts (Yakovleva and Emneus 2008). Immunosensors are classified in competitive and non-competitive assays (The Immunoassay Handbook. Theory and Applications of Ligand Binding, ELISA and Related Techniques 2013). Figure 2.9a depicts a “sandwich-type” immunoassay. This is a non-competitive assay, and represents the most common immunosensor type. Here, the biosensor contains a capture antibody that, in contact with the sample, reacts with the target analyte, binding it. After a certain reaction period, the biosensor with the captured antigen is washed, and made to react with a medium containing a labelled secondary antibody. After the necessary reaction time, the biosensor is washed again, and introduced in a solution containing the substrate for the enzymatic label. At this stage, the detection is based on monitoring the activity of the enzymatic label. The more analyte in the sample, the more signal is recorded.

Competitive immunoassays (Fig. 2.9b) consist in the competition of the target analyte and a labelled version of the analyte, and generally used when matched antibodies against the target analyte are not available or in the detection of small molecules. The maximum signal is obtained in the absence of analyte, and as the concentration of analyte increases the biosensor signal decreases because the affinity of the antibody is greater for the analyte than for its labelled version. Competitive assays are usually harder to develop than non-competitive ones because the relative concentrations of the labelled antigen and the target analyte have to be carefully adjusted.

These two types of immunosensor rely on enzymatic labels. However, label-less immunosensors are also possible as long as the detection method can detect the antigen-antibody interaction directly. Examples of these are biosensors based on quartz crystal microbalance (QCM) (Ben-Dov et al. 1997), surface plasmon resonance (SPR) (Shankaran et al. 2007), and electrochemical impedance spectroscopy (EIS) (Bart et al. 2005).

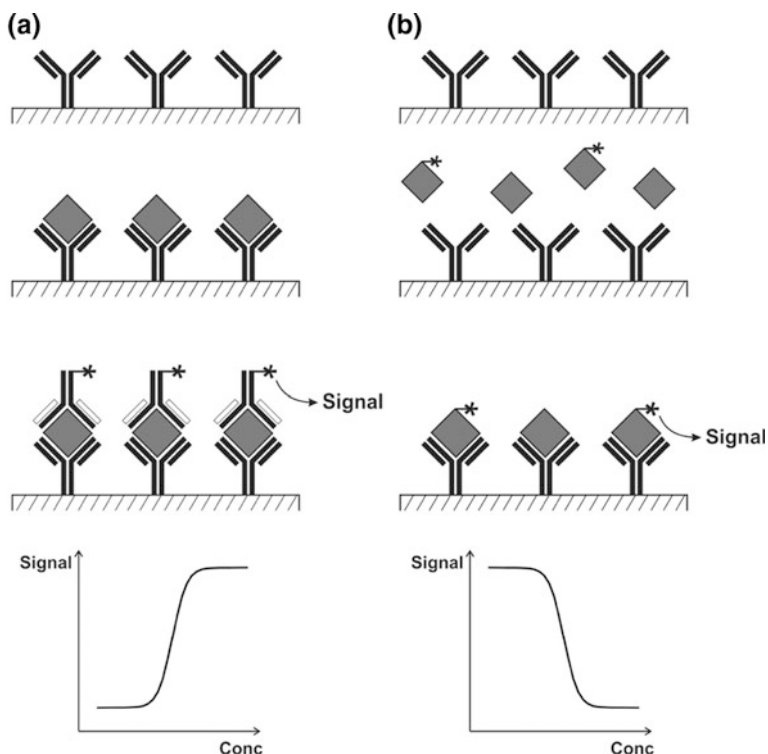


Fig. 2.9 Schematic depiction of the different types of immunoassays. **a** Non-competitive immunoassay in which the sample is incubated with the antibodies attached to a surface. After a washing step, a second antibody bind the antigen (Sandwich type) and a signal is recorded. **b** Example of a competitive immunoassay where the antigen in the sample is incubated with labelled antigen and they compete to bind the antibody

2.4.4 On Biosensor Performance

Biosensors pose different, often much more complex, challenges than physical sensors, and their lifetime is typically much shorter. Biosensor performance deteriorates over time due to causes such as biorecognition element activity loss, fouling, and other factors associated to the conditions of use, such as sample nature, and changes in temperature, humidity or pH can have a significant impact on results. Therefore, when developing biosensors for use at the point of care, a number of important considerations need to be made.

Point of care devices may be used both by lay persons and healthcare professionals, but the specific requirements differ from one type of usage setting to another. Thus, when devices are intended for use in a professional setting, the user profile and specific performance parameters need to be clearly defined. In contrast, the development of medical devices for home users requires an additional focus on

safety, particularly in the control of infections arising from improper use (sharing between users without effective cleaning) of meters and lancing devices. The Food and Drug Administration in the US have issued separate guidance documents to address the development of glucose monitoring devices adapted to different user types (FDA 2016a, b).

The performance testing for point of care biosensors is exhaustive and affects both biosensor and instrumentation and software. However, this section focuses on analytical aspects such as desirable precision and accuracy, repeatability, interference studies, and data analysis and presentation of results.

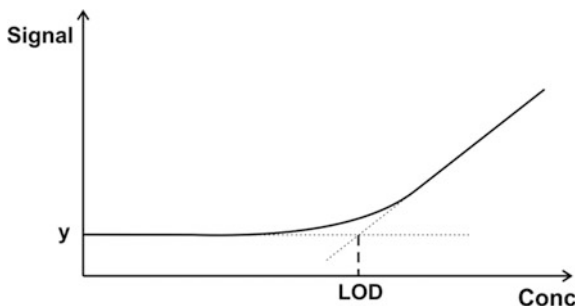
2.4.5 *Bisensor Linear Range and Calibration Issues*

Any analytical method is valid only within its own specific and well-defined conditions. The calibration of a sensor consists in establishing the relation between the signal measured by the system and the analyte concentration present in a set of standards. The detection limit is the minimum concentration that can be detected unambiguously from the background signal, and its most common definitions are those provided by the IUPAC (Mocak et al. 1997) and the ACS (Winefordner 2016). (1) The limit of detection, expressed as a concentration or quantity, is derived from the smallest measure that can be detected with reasonable certainty for a given analytical procedure (IUPAC), and (2) The limit of detection is the lowest concentration of an analyte that the analytical process can reliably detect (ACS). Similarly, the RSC defines “the detection limit of an analytical procedure is regarded as being the lowest concentration of the analyte that can be distinguished with reasonable confidence from a *field blank*” (Analytical Methods 1987).

The detection limit can be determined graphically by plotting the transducer signal against the concentration of analyte, and finding the intersect between the extrapolation of the linear region and the baseline. Another way of looking at the detection limit is to see it as the concentration corresponding to the minimum signal that is significantly different from the background signal in the absence of analyte. This is depicted in Fig. 2.10. This figure presents the common methodology known as the 3 s method, which defines the detection limit as the concentration which signal $y = y_B + 3s_B$, where y_B is the average background signal, and s_B corresponds to the standard deviation of the y -residuals from the line of best fit (within the linear response region).

While this second method is perhaps more common in the scientific literature, Long and Winefordner showed that this method occasionally leads to falsely low detection limits (Winefordner 2016), particularly when the main source of error is in the blank, and proposed a more robust methodology based on the propagation of errors.

Fig. 2.10 Representation of a standard calibration curve where the intercept of the two linear zones determines an assay detection limit



In the case of enzymatic biosensors, the system response matches the Michaelis-Menten type curves presented above, and the linear region is limited by the Michaelis constant (K_m). This linear region, however, may be extended through the use of diffusional barriers (Leddy et al. 1985; Mullen et al. 1986). These diffusional barriers are permeable membranes which role is to slow down the access of the target analyte into the biosensor. Ideally, these membranes may also provide other benefits, such as the stabilization of enzymes, or the protection against fouling and possible interfering agents. This is the case, for instance, of Nafion membranes, which are routinely used to block anionic electroactive species such as ascorbic and uric acid (Wang 2008).

However, the introduction of diffusion barriers results in increased response times (Mullen et al. 1986). Response times up to 60 s are acceptable for biosensors at the point of care, so it is important to reach a compromise between linearity, sensitivity, and response time.

The fact that most biosensors are intended for single use complicates their calibration compared to other electrochemical sensors, i.e.: pH electrodes, which can be calibrated many times throughout their life using adequate standards. Typical calibration procedures differ from one sensor type to another. Ideally, calibrations should involve multiple point testing. However, single point calibration is accepted in cases in which only one measurement point is required. This is provided that the sensitivity is known and that the response is linear in the desired measurement range, as in the case of certain potentiometric measurements (Lindner and Umezawa 2008).

Biosensors are rarely calibrated at the point-of-care. Instead, they are calibrated per batch at the factory, and the corresponding calibration data is introduced in the instrument with each biosensor lot. One way of doing this is to provide a chip with the factory calibration information with each biosensor lot (Matteucci et al. 2014; Shephard et al. 2007). Another approach is to insert a code number in the instrument to adjust it to the new biosensor batch.

Table 2.1 Glucose concentration intervals of interest in the development of self monitoring blood glucose test devices

Interval	Glucose concentration range/mg dL ⁻¹
1	30–50
2	51–110
3	111–150
4	151–250
5	251–400

2.4.6 Samples and Concentration Ranges

The concentration range of biological interest is split in sub-ranges of clinical importance. In the case of glucose, the 5 concentration intervals shown in Table 2.1 need to be considered.

When no real samples can be obtained to represent one of these intervals, an available sample may be diluted or spiked accordingly so that the entire concentration range can be studied, and all alterations need to be reported.

2.4.7 Accuracy and Precision

Accuracy is determined by comparison of the biosensor response to different analyte concentration intervals against an accepted reference method. In the case of glucose, typically 5 concentration intervals are chosen to reflect low, normal, and high glucose concentration levels. The reference method normally works on venous blood samples so, depending on the nature of the assay under developed, there are bound to be differences between the test and the reference methods. However, despite these differences, there should be a correlation between both datasets, and these are assessed so-called Consensus error grids (Parkes et al. 2000), as depicted in Fig. 2.11. The consensus error grid is a modern version of Clarke's error grid, which defined different zones in his plot to assess glucose meters (Clarke et al. 1987, 2008; Cox et al. 1985; Hasslacher et al. 2013). The implications of the different areas are summarized in Table 2.2.

If the test method falls within 20% of the reference method, then the point belongs to zone A. Points with greater than 20% deviation but which would lead to no adverse treatment by the patient would fall under zone B. If the glucose concentration is normal according to the reference method, but the meter result is outside the range, then the point falls within C. Results in this region may lead to patients receiving treatment unnecessarily, because the glucose concentration is normal. Zone D represents those results where the reference method gives an abnormal glucose reading whilst the test method reports a normal level, resulting in the patient not receiving adequate treatment. Last, if the glucose concentration is actually high but the test method reports a low value, or vice versa, then the point falls within zone E. In this region, the treatment given to the patient is actually the

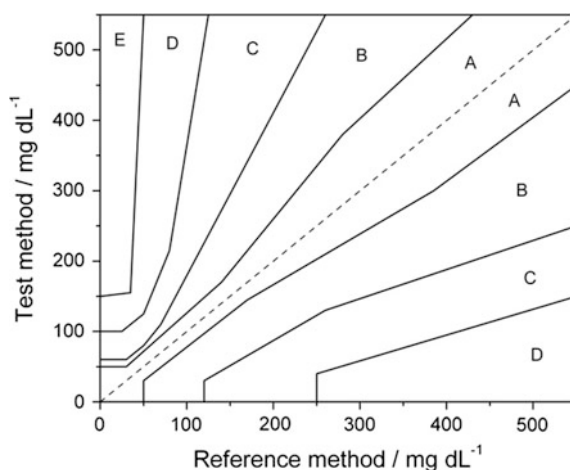


Fig. 2.11 Consensus error grid for glucose monitoring devices. Taken from ISO 15197:2013 (AENOR 2013)

Table 2.2 Definition of error zones in the consensus diagram according to ISO 15197:2003 (AENOR 2013)

Consensus error zone	Risk to patient
A	No effect on clinical action
B	Altered clinical action—little or no effect on clinical outcome
C	Altered clinical action—likely to affect clinical outcome
D	Altered clinical action—could have significant medical risk
E	Altered clinical action—could have dangerous consequences

opposite from what would be required, and severe health damage is likely. The accuracy requirements are very strict in the case of glucose, and 99% of the values are required to be within zones A and B.

Precision is reported in terms of variance coefficient percentage or in $\pm \text{mg dL}^{-1}$. The goal is to achieve precisions better than 5% CV. In reality, the errors tend to be greater in the low concentration range because of electrical noise at low current levels. Precision testing is normally done at two different levels: within-run and intermediate. *Within-run* precision testing are designed to determine precision under conditions of repeated testing of the same sample using different meters and biosensors from multiple lots. Samples within all of the relevant concentration intervals, i.e. in the case of glucose, those presented in Table 2.3, need to be included in these tests. *Intermediate* precision testing, on the other hand, aims to evaluate precision under simulated normal use conditions, and they may be performed using control solutions rather than real samples. One common case of intermediate precision testing assesses the precision of a number of meters using

Table 2.3 A list of common interfering substances to consider in the development of glucose biosensors for clinical use

Interferant	Recommended test concentration	Interferant	Recommended test concentration
Acetaminophen	20 mg dL ⁻¹	Ibuprofen	50 mg dL ⁻¹
Ascorbic acid	3 mg dL ⁻¹	Icodextrin	1094.4 mg dL ⁻¹
Conjugated bilirubin	50 mg dL ⁻¹	L-Dopa	0.5 mg dL ⁻¹
Unconjugated bilirubin	50 mg dL ⁻¹	Maltose	10,000 mg dL ⁻¹
Cholesterol	500 mg dL ⁻¹	Methyldopa	1000 mg dL ⁻¹
Creatinine	10 mg dL ⁻¹	Salicylic acid	60 mg dL ⁻¹
Dopamine	20 mg dL ⁻¹	Sodium	414 mg dL ⁻¹
EDTA	200 mg dL ⁻¹	Tolbutamide	100 mg dL ⁻¹
Galactose	15 mg dL ⁻¹	Tolazamide	40 mg dL ⁻¹
Gentisic acid	1000 mg dL ⁻¹	Triglycerides	1500 mg dL ⁻¹
Reduced Glutathione	92 mg dL ⁻¹	Uric acid	24 mg dL ⁻¹
Hemoglobin	20 g dL ⁻¹	Xylose	200 mg dL ⁻¹
Heparin	500 IU/dL ⁻¹	Sugar alcohols	0.09 mg dL ⁻¹

biosensors from several batches at all the relevant concentration intervals over a minimum period of 10 days.

The linearity of the biosensor response also needs to be studied. A minimum number of 11 evenly spaced points is recommended (CLSI 2003).

2.4.8 Interference Testing

The effect of potential interfering endogenous and exogenous conditions on the device performance needs to be examined. Interference testing needs to be carried out at all relevant concentration intervals within the device range, with a focus on concentrations of particular clinical relevance. These tests should include the interfering agents at the maximum concentration that they could be found in the target sample. When interference is found, dilutions need to be carried out to identify the concentration at which interference begins to occur. Table 2.3 lists the common interfering agents identified by the FDA, and which are of interest in blood glucose testing.

2.4.9 Biosensor Stability Testing

Shelf life, or the time span a product remains usable after manufacture, is a key performance parameter in biosensors, but more importantly so when the health of users depends on it. Biosensor performance needs to be assessed throughout the claimed biosensor lifetime. These tests should be performed under three different set of conditions: (i) closed vial stability or shelf-life, (ii) open vial stability through to the recommended expiry date, and (iii) extended open vial stability. This is a test that simulates the case in which a vial has been left open for the entire claimed lifetime of the biosensor, and should aim to cover a wide range of temperature and humidity conditions. In each of these tests, accuracy and precision needs to be assessed for each of the relevant concentration interval.

2.5 Outlook: Electrochemical Biosensors at the Point of Care

Biosensors are complex analytical devices in constant evolution. The most important biosensor, at least by market value, continues to be the glucose one. Other enzymatic biosensors are also available. These are usually based on oxidases and quantification of the target analyte is done through the peroxide produced in their reaction. Despite the large volume of new publications addressing biosensors each year (around 5000 according to Scopus), the number of commercially available devices based on biosensors is shockingly small. One of the main reasons for this is manufacturability or, rather, the lack of it in most new developments. A second hurdle may be found in the cost and effort involved in the development of those biosensors into user-friendly products, which involve not only the development of the biosensors themselves, but also the instrumentation and software around them. Another obstacle is cost of validation and certification. This is particularly true in the case of devices aimed at point-of-care use, regardless of whether intended for lay persons or healthcare professionals, as the regulations impose very strict controls and very high levels of robustness and reliability are demanded. Commercialization and distribution of new (medical) products poses an additional hurdle, and market penetration and user acceptance impose yet more difficulties. The success of the glucose biosensor stems from the huge importance of diabetes as a chronic disease affecting over 10% of the world population, which more than justifies the investment. The glucose biosensor has enjoyed the benefits of miniaturization and advances in different areas of technology, going from benchtop laboratory instrument to the ubiquitous glucometers for self-testing. The trend nowadays is moving towards non-invasive methods of analysis, aiming to improve the quality of life of chronic patients. Abbott's Freestyle Libre glucose monitor, recently studied by Bailey et al. (2015) is still considered invasive since it monitors the concentration of glucose in interstitial fluid through a small needle, but it can be

worn for up to 14 days during which regular readings (up to every 15 min) can be taken easily by means of a wireless reader, without the need for fingerstick measurements.

Several research groups are developing *wearable* sensors (Ajami and Teimouri 2015; Crean et al. 2012; Kuehn 2016), mostly in the form of skin-patches with more or less complexity (Heikenfeld 2016; Jia et al. 2013; Lee et al. 2017; Rose et al. 2015; Windmiller et al. 2012). This new wave of devices will doubtlessly bring multiple benefits both to patients and to the healthcare system, but they are still a few years away from the market. These new wearable devices will need to provide reliable measurements, but they will also have to allow the easy management of their information, both by the user and by the healthcare professional.

Acknowledgement This chapter was prepared in collaboration with Miguel Aller.

References

- AENOR (2013) ISO 15197:2013 in vitro diagnostic test systems—requirements for blood-glucose monitoring systems for self-testing in managing diabetes mellitus
- Ajami S, Teimouri F (2015) Features and application of wearable biosensors in medical care. *J Res Med Sci* 20:1208–1215
- Albery J (1975) *Electrode kinetics*. Oxford chemistry series. Clarendon Press, Oxford
- Albery JW, Hitchman ML (1971) *Ring-disc electrodes*. Clarendon Press, Oxford
- Amatore C (1995) Electrochemistry at ultramicroelectrodes. In: Rubinstein I (ed) *Physical electrochemistry: science and technology*. Marcel Dekker, New York, pp 131–208
- Amatore C, Maisonhaute E, Simonneau G (2000) Ohmic drop compensation in cyclic voltammetry at scan rates in the megavolt per second range: access to nanometric diffusion layers via transient electrochemistry. *J Electroanal Chem* 486:141–155
- Amine A, Mohammadi H, Bourais I, Palleschi G (2006) Enzyme inhibition-based biosensors for food safety and environmental monitoring. *Biosens Bioelectron* 21:1405–1423
- Analytical Methods C (1987) Recommendations for the definition, estimation and use of the detection limit. *Analyst* 112:199–204
- Andrieux CP, Dumas-Bouchiat JM, Saveant JM (1978) Homogeneous redox catalysis of electrochemical reactions. Part I. Introduction. *J Electroanal Chem* 87:39–53
- Arrigan DWM (2004) Nanoelectrodes, nanoelectrode arrays and their applications. *Analyst* 129:1157–1165
- Arya SK, Datta M, Malhotra BD (2008) Recent advances in cholesterol biosensor. *Biosens Bioelectron* 23:1083–1100
- Azevedo AM, Prazeres DMF, Cabral JMS, Fonseca LP (2005) Ethanol biosensors based on alcohol oxidase. *Biosens Bioelectron* 21:235–247
- Bailey T, Bode BW, Christiansen MP, Klaff LJ, Alva S (2015) The performance and usability of a factory-calibrated flash glucose monitoring system. *Diabetes Technol Ther* 17:787–794
- Banks CE, Compton RG (2003) Sono-electroanalysis: a review. *Chem Anal (Warsaw)* 48:159–180
- Banks CE et al (2003) Electrochemistry of immobilised redox droplets: concepts and applications. *PCCP* 5:4053–4069
- Barbir F (2013) *PEM fuel cells*. Elsevier Inc
- Bard AJ, Faulkner LR (2001) *Electrochemical methods: fundamentals and applications*. Wiley, New York

- Barsoukov E, Macdonald JR (2005) Impedance spectroscopy: theory, experiment, and applications. Wiley-Interscience, Hoboken
- Bart M, Stigter ECA, Stapert HR, De Jong GJ, Van Bennekom WP (2005) On the response of a label-free interferon- γ immunosensor utilizing electrochemical impedance spectroscopy. *Biosens Bioelectron* 21:49–59
- Ben-Dov I, Willner I, Zisman E (1997) Piezoelectric immunosensors for urine specimens of chlamydia trachomatis employing quartz crystal microbalance microgravimetric analyses. *Anal Chem* 69:3506–3512
- Benito-Peña E, Valdés MG, Glahn-Martínez B, Moreno-Bondi MC (2016) Fluorescence based fiber optic and planar waveguide biosensors. A review. *Anal Chim Acta* 943:17–40
- Biosensors and Bioelectronics (2017) Elsevier. <https://www.journals.elsevier.com/biosensors-and-bioelectronics>
- Bond AM (1994) Past, present and future contributions of microelectrodes to analytical studies employing voltammetric detection. A review. *Analyst* 119:R1–R21
- Bond AM, Fleischmann M, Robinson J (1984) Electrochemistry in organic solvents without supporting electrolyte using platinum microelectrodes. *J Electroanal Chem* 168:299–312
- Buck RP, Lindner E (1994) Recommendations for nomenclature of ionselective electrodes (IUPAC Recommendations 1994). *Pure Appl Chem* 66:2527–2536
- Burcu Bahadır E, Kemal Sezgintürk M (2015) Applications of electrochemical immunosensors for early clinical diagnostics. *Talanta* 132:162–174
- Chapman DL (1910) A contribution to the theory of electrocapillarity. *Phil Mag* 25:475–481
- Chikkaveeraiah BV, Bhirde AA, Morgan NY, Eden HS, Chen X (2012) Electrochemical immunosensors for detection of cancer protein biomarkers. *ACS Nano* 6:6546–6561
- Clarke WL, Anderson S, Kovatchev B (2008) Evaluating clinical accuracy of continuous glucose monitoring systems: continuous glucose—error grid analysis (CG-EGA). *Current Diabetes Reviews* 4:193–199
- Clarke WL, Cox D, Gonder-Frederick LA, Carter W, Pohl SL (1987) Evaluating clinical accuracy of systems for self-monitoring of blood glucose. *Diabetes Care* 10:622–628
- Clausmeyer J, Schuhmann W (2016) Nanoelectrodes: applications in electrocatalysis, single-cell analysis and high-resolution electrochemical imaging. *TrAC—Trends Anal Chem* 79:46–59
- CLSI (2003) Evaluation of the linearity of quantitative measurement procedures: a statistical approach. CLSI document EP06-A. Clinical and Laboratory Standards Institute, Wayne, PA
- Compton RG, Banks CE (2010) Understanding voltammetry. World Scientific, Singapore
- Compton RG, Eklund JC, Marken F (1997) Sonoelectrochemical processes: a review. *Electroanalysis* 9:509–522
- Compton RG, Sanders GHW (1996) Electrode potentials, vol 41. Oxford University Primers. Oxford University Press, Oxford
- Cooper JA, Compton RG (1998) Channel electrodes—a review. *Electroanalysis* 10:141–155
- Cooper MA, Singleton VT (2007) A survey of the 2001 to 2005 quartz crystal microbalance biosensor literature: applications of acoustic physics to the analysis of biomolecular interactions. *J Mol Recognit* 20:154–184
- Cornish-Bowden A (2011) Fundamentals of enzyme kinetics. Wiley-Blackwell, Singapore
- Costentin C, Robert M, Savéant JM (2006) Electron transfer and bond breaking: recent advances. *Chem Phys* 324:40–56
- Cox DJ et al (1985) Accuracy of perceiving blood glucose in IDDM. *Diabetes Care* 8:529–536
- Crean C, McGeough C, O’Kennedy R (2012) Wearable biosensors for medical applications. In: *Biosensors for medical applications*. Elsevier Inc., pp 301–330
- Cussler EL (2009) Diffusion: mass transfer in fluid systems, 3rd edn
- Dequaire M, Limoges B, Moiroux J, Savéant JM (2002) Mediated electrochemistry of horseradish peroxidase. Catalysis and inhibition. *J Am Chem Soc* 124:240–253
- Economou A, Kokkinos C (2016) Chapter 1: Advances in stripping analysis of metals, vol 2016-January. Royal Society of Chemistry
- Eggins BR (2002) Chemical sensors and biosensors. Wiley, Hoboken

- Fda U (2016a) Blood glucose monitoring test systems for prescription point-of-care use. US FDA, Rockville
- Fda U (2016b) Self-monitoring blood glucose test systems for over-the-counter use. US FDA, Rockville
- Fortgang P, Amatore C, Maisonhaute E, Schöllhorn B (2010) Microchip for ultrafast voltammetry. *Electrochem Commun* 12:897–900
- Fu F, Wang Q (2011) Removal of heavy metal ions from wastewaters: a review. *J Environ Manag* 92:407–418
- Gabrielli C (1995) Electrochemical impedance spectroscopy: principles, instrumentation, and applications. In: Rubinstein I (ed) *Physical electrochemistry: science and technology*. Marcel Dekker, New York, pp 243–291
- Garjonyte R, Yigzaw Y, Meskys R, Malinauskas A, Gorton L (2001) Prussian Blue- and lactate oxidase-based amperometric biosensor for lactic acid. *Sens Actuators B: Chem* 79:33–38
- Garreau D, Savéant JM (1972) Linear sweep voltammetry-compensation of cell resistance and stability. Determination of the residual uncompensated resistance. *J Electroanal Chem* 35:309–331
- Godino N, Borrisse X, Xavier Munoz F, Javier del Campo F, Compton RG (2009) Mass transport to nanoelectrode arrays and limitations of the diffusion domain approach: theory and experiment. *J Phys Chem C* 113:11119–11125
- Goedhart J, Hink MA, Jalink K (2014) An introduction to fluorescence imaging techniques geared towards biosensor applications, vol 1071. Humana Press Inc
- Gorton L, Jönsson-Pettersson G, Csöregi E, Johansson K, Dominguez E, Marko-Varga G (1992) Amperometric biosensors based on an apparent direct electron transfer between electrodes and immobilized peroxidases plenary lecture. *Analyst* 117:1235–1241
- Gorton L, Lindgren A, Larsson T, Munteanu FD, Ruzgas T, Gazaryan I (1999) Direct electron transfer between heme-containing enzymes and electrodes as basis for third generation biosensors. *Anal Chim Acta* 400:91–108
- Gosser DK (1993) *Cyclic voltammetry. Simulation and analysis of reaction mechanisms*. Wiley-VCH
- Gouy G (1910a) *Compt Rend* 149:654
- Gouy G (1910b) *J Phys Radium* 9:457
- Grahame DC (1947) The electrical double layer and the theory of electrocapillarity. *Chem Rev* 41:441–501
- Gründler P, Kirbs A, Zerihun T (1996) Hot-wire electrodes: voltammetry above the boiling point. *Analyst* 121:1805–1810
- Guidelli R, Compton RG, Feliu JM, Gileadi E, Lipkowski J, Schmickler W, Trasatti S (2014) Definition of the transfer coefficient in electrochemistry (IUPAC Recommendations 2014). *Pure Appl Chem* 86
- Habermüller K, Mosbach M, Schuhmann W (2000) Electron-transfer mechanisms in amperometric biosensors. *Fresenius' J Anal Chem* 366:560–568
- Hasslacher C, Kulozik F, Platten I (2013) Accuracy of self monitoring blood glucose systems in a clinical setting: application of new planned ISO-Standards. *Clin Lab* 59:727–733
- Heikenfeld J (2016) Bioanalytical devices: technological leap for sweat sensing. *Nature* 529:475–476
- Heinze J (1993) Ultramicroelectrodes in electrochemistry. *Angew Chem Int Ed Engl* 32:1268–1288
- Heller A (1990) Electrical wiring of redox enzymes. *Acc Chem Res* 23:128–134
- Helmholtz H (1853) Ueber einige Gesetze der Vertheilung elektrischer Ströme in körperlichen Leitern mit Anwendung auf die thierisch-elektrischen Versuche *Annalen der Physik und Chemie* 165:211–233
- Henstridge MC, Laborda E, Rees NV, Compton RG (2012) Marcus-Hush-Chidsey theory of electron transfer applied to voltammetry: a review. *Electrochim Acta* 84:12–20
- Herzog G, Beni V (2013) Stripping voltammetry at micro-interface arrays: a review. *Anal Chim Acta* 769:10–21

- Howell JO, Wightman RM (1984) Ultrafast voltammetry and voltammetry in highly resistive solutions with microvoltammetric electrodes. *Anal Chem* 56:524–529
- Hulbert MH, Shain I (1970) Rate-controlled adsorption of product in stationary electrode polarography. *Anal Chem* 42:162–171
- The Immunoassay Handbook (2013) Theory and applications of ligand binding, ELISA and related techniques, 4th edn. Elsevier Science
- Inzelt G, Lewenstam A, Scholz F (2013) Handbook of reference electrodes. Springer, Berlin, Heidelberg
- Jia W et al (2013) Electrochemical tattoo biosensors for real-time noninvasive lactate monitoring in human perspiration. *Anal Chem* 85:6553–6560
- Karyakin AA, Gitelmacher OV, Karyakina EE (1995) Prussian blue-based first-generation biosensor. A sensitive amperometric electrode for glucose. *Anal Chem* 67:2419–2423
- Katz E, Willner I (2003) Probing biomolecular interactions at conductive and semiconductive surfaces by impedance spectroscopy: routes to impedimetric immunosensors, DNA-sensors, and enzyme biosensors. *Electroanalysis* 15:913–947
- Kuehn BM (2016) Wearable biosensors studied for clinical monitoring and treatment. *JAMA—J Am Med Assoc* 316:255–257
- Laocharoensuk R (2016) Development of electrochemical immunosensors towards point-of-care cancer diagnostics: clinically relevant studies. *Electroanalysis* 28:1716–1729
- Lauks IR (1990) Reference electrode, method of making and method of using same. US Patent
- Leddy J, Bard AJ, Maloy JT, Savéant JM (1985) Kinetics of film-coated electrodes. Effect of a finite mass transfer rate of substrate across the film-solution interface at steady state. *J Electroanal Chem* 187:205–227
- Lee H et al (2017) Wearable/disposable sweat-based glucose monitoring device with multistage transdermal drug delivery module. *Sci Adv* 3:e1601314
- Levich V (1962) Physicochemical hydrodynamics. Prentice Hall, London
- Lim SA, Ahmed MU (2016) Electrochemical immunosensors and their recent nanomaterial-based signal amplification strategies: a review. *RSC Adv* 6:24995–25014
- Limon-Petersen JG, Han JT, Rees NV, Dickinson EJJ, Streeter I, Compton RG (2010) Quantitative voltammetry in weakly supported media. chronoamperometric studies on diverse one electron redox couples containing various charged species: dissecting diffusional and migrational contributions and assessing the breakdown of electroneutrality. *J Phys Chem C* 114:2227–2236
- Limon-Petersen JG, Streeter I, Rees NV, Compton RG (2009) Quantitative voltammetry in weakly supported media: effects of the applied overpotential and supporting electrolyte concentration on the one electron oxidation of ferrocene in acetonitrile. *J Phys Chem C* 113:333–337
- Lindner E, Umezawa Y (2008) Performance evaluation criteria for preparation and measurement of macro- and microfabricated ion-selective electrodes (IUPAC Technical Report). *Pure Appl Chem* 80:85–104
- Lojou É, Bianco P (2004) Membrane electrodes for protein and enzyme electrochemistry. *Electroanalysis* 16:1113–1121
- Lovrić M (2010) Stripping voltammetry. *Electroanalytical methods: guide to experiments and applications*. Springer, Berlin Heidelberg, pp 201–221
- March G, Nguyen TD, Piro B (2015) Modified electrodes used for electrochemical detection of metal ions in environmental analysis. *Biosensors* 5:241–275
- Martínez-Huitle CA, Ferro S (2006) Electrochemical oxidation of organic pollutants for the wastewater treatment: direct and indirect processes. *Chem Soc Rev* 35:1324–1340
- Matsuda H, Ayabe Y (1955) Zur Theorie der Randles-Sevcik schen Kathodenstrahl-Polarographie *Z Elektrochem* 59:494–503
- Matteucci E, Della Bartola L, Rossi L, Pellegrini G, Giampietro O (2014) Improving CardioCheck PA analytical performance: three-year study. *Clin Chem Lab Med* 52:1291–1296
- Minunni M, Mascini M, Guilbault GG, Hock B (1995) The quartz crystal microbalance as biosensor. A status report on its future. *Anal Lett* 28:749–764

- Mocak J, Bond AM, Mitchell S, Scollary G (1997) A statistical overview of standard (IUPAC and ACS) and new procedures for determining the limits of detection and quantification: application to voltammetric and stripping techniques. *Pure Appl Chem* 69:297–328
- Mulchandani A, Rogers KR (eds) (1998) Enzyme and microbial biosensors. *Methods in biotechnology*. Humana Press, Totowa
- Mullen WH, Keedy FH, Churchouse SJ, Vadgama PM (1986) Glucose enzyme electrode with extended linearity. *Anal Chim Acta* 183:59–66
- Ngamchuea K, Eloul S, Tschulik K, Compton RG (2014) Planar diffusion to macro disc electrodes —what electrode size is required for the Cottrell and Randles-Sevcik equations to apply quantitatively? *J Solid State Electrochem* 18:3251–3257
- Nicholson RS (1965) Theory and application of cyclic voltammetry for measurement of electrode reaction kinetics. *Anal Chem* 37:1351–1355
- Nicholson RS, Shain I (1964) Theory of stationary electrode polarography. Single scan and cyclic methods applied to reversible, irreversible, and kinetic systems. *Anal Chem* 36:706–723
- Olaru A, Bala C, Jaffrezic-Renault N, Aboul-Enein HY (2015) Surface plasmon resonance (SPR) biosensors in pharmaceutical analysis. *Crit Rev Anal Chem* 45:97–105
- Oldham KB (1979) Analytical expressions for the reversible Randles-Sevcik function. *J Electroanal Chem* 105:373–375
- Orazem ME, Tribollet B (2011) Electrochemical impedance spectroscopy. Wiley-Interscience
- Parkes JL, Slatin SL, Pardo S, Ginsberg BH (2000) A new consensus error grid to evaluate the clinical significance of inaccuracies in the measurement of blood glucose. *Diabetes Care* 23:1143–1148
- Parsons R (1974) Electrochemical nomenclature. *Pure Appl Chem* 37:499–516
- Pilling MJ, Seakins PW (1995) Reaction kinetics. Oxford University Press
- Pistoia G (2014) Lithium-ion batteries: advances and applications. *Lithium-ion batteries: advances and applications*. Elsevier BV
- Rama EC, Costa-García A (2016) Screen-printed Electrochemical Immunosensors for the detection of cancer and cardiovascular biomarkers. *Electroanalysis* 28:1700–1715
- Ronkainen NJ, Halsall HB, Heineman WR (2010) Electrochemical biosensors. *Chem Soc Rev* 39:1747–1717
- Rose DP et al (2015) Adhesive RFID sensor patch for monitoring of sweat electrolytes. *IEEE Trans Biomed Eng* 62:1457–1465
- Sadana A, Sadana N (2010) Handbook of biosensors and biosensor kinetics. Elsevier Science
- Savéant JM (2000) Electron transfer, bond breaking and bond formation, vol 35
- Savéant JM (2008) Molecular catalysis of electrochemical reactions. Mechanistic aspects. *Chem Rev* 108:2348–2378
- Schäfer HJ (2011) Contributions of organic electrosynthesis to green chemistry. *C R Chim* 14:745–765
- Scheller FW et al (1991) Second generation biosensors. *Biosens Bioelectron* 6:245–253
- Scholz F (2010) Electroanalytical Methods. Guide to experiments and applications. Springer
- Schultze JW, Bressel A (2001) Principles of electrochemical micro- and nano-system technologies. *Electrochim Acta* 47:3–21
- Scrosati B, Garche J (2010) Lithium batteries: Status, prospects and future. *J Power Sources* 195:2419–2430
- Shankaran DR, Gobi KV, Miura N (2007) Recent advancements in surface plasmon resonance immunosensors for detection of small molecules of biomedical, food and environmental interest. *Sens Actuators B: Chem* 121:158–177
- Shephard MDS, Mazzachi BC, Shephard AK (2007) Comparative performance of two point-of-care analysers for lipid testing. *Clin Lab* 53:561–566
- Shoup D, Szabo A (1982) Chronoamperometric current at finite disk electrodes. *J Electroanal Chem Interfacial Electrochem* 140:237–245

- Singh S, Solanki PR, Pandey MK, Malhotra BD (2006) Cholesterol biosensor based on cholesterol esterase, cholesterol oxidase and peroxidase immobilized onto conducting polyaniline films. *Sens Actuators B: Chem* 115:534–541
- Sirkar K, Revzin A, Pishko MV (2000) Glucose and lactate biosensors based on redox polymer/oxidoreductase nanocomposite thin films. *Anal Chem* 72:2930–2936
- Snowden ME, King PH, Covington JA, MacPherson JV, Unwin PR (2010) Fabrication of versatile channel flow cells for quantitative electroanalysis using prototyping. *Anal Chem* 82:3124–3131
- Stern O (1924) Zur theorie der elektrolytischen doppelschicht *Zeitschrift für Elektrochemie und angewandte physikalische Chemie* 30:508–516
- Stoica L, Ludwig R, Haltrich D, Gorton L (2006) Third-generation biosensor for lactose based on newly discovered cellobiose dehydrogenase. *Anal Chem* 78:393–398
- Štulík K, Amatore C, Holub K, Mareček V, Kutner W (2000) Microelectrodes. Definitions, characterization, and applications (Technical report). *Pure Appl Chem* 72:1483–1492
- Taurino I et al (2016) Recent advances in third generation biosensors based on Au and Pt nanostructured electrodes. *TrAC—Trends Anal Chem* 79:151–159
- Trojanowicz M (2009) Recent developments in electrochemical flow detections—a review. Part I. Flow analysis and capillary electrophoresis. *Anal Chim Acta* 653:36–58
- Turner APF (1987) Karube I. In: Wilson GS (eds) *Biosensors, fundamentals and applications*
- Turner APF (2013) Biosensors: sense and sensibility. *Chem Soc Rev* 42:3184
- Urdike SJ, Hicks GP (1967) The enzyme electrode. *Nature* 214:986–988
- Varfolomeev SD, Kurochkin IN, Yaropolov AI (1996) Direct electron transfer effect biosensors. *Biosens Bioelectron* 11:863–871
- Vashist SK, Luong JHT (2015) Recent advances in electrochemical biosensing schemes using graphene and graphene-based nanocomposites. *Carbon* 84:519–550
- Vijayakumar AR, Csöregi E, Heller A, Gorton L (1996) Alcohol biosensors based on coupled oxidase-peroxidase systems. *Anal Chim Acta* 327:223–234
- Wan Y, Su Y, Zhu X, Liu G, Fan C (2013) Development of electrochemical immunosensors towards point of care diagnostics. *Biosens Bioelectron* 47:1–11
- Wang J (2000) *Analytical electrochemistry*. Wiley-VCH, New York
- Wang J (2008) Electrochemical glucose biosensors. *Chem Rev* 108:814–825
- Willner I, Yan YM, Willner B, Tel-Vered R (2009) Integrated enzyme-based biofuel cells—a review. *Fuel Cells* 9:7–24
- Windmiller JR, Bhandekar AJ, Valdés-Ramírez G, Parkhomovskiy S, Martínez AG, Wang J (2012) Electrochemical sensing based on printable temporary transfer tattoos. *Chem Commun* 48:6794–6793
- Winefordner GLLJD (2016) Limit of detection. A closer look at the IUPAC definition, pp 1–13
- Winter M, Brodd RJ (2004) What are batteries, fuel cells, and supercapacitors? *Chem Rev* 104:4245–4269
- Wu L, Zhang X, Chen J (2014) A new third-generation biosensor for superoxide anion based on dendritic gold nanostructure. *J Electroanal Chem* 726:112–118
- Xu SX, Li JL, Zhou ZL, Zhang CX (2014) A third-generation hydrogen peroxide biosensor based on horseradish peroxidase immobilized by sol-gel thin film on a multi-wall carbon nanotube modified electrode. *Anal Methods* 6:6310–6315
- Yakovleva J, Emneus J (2008) Electrochemical Immunosensors. In: Bartlett PN (ed) *Bioelectrochemistry: fundamentals, experimental techniques and applications*. Wiley, Chichester, pp 377–410
- Yarman A et al (2011) Can peroxxygenase and microperoxidase substitute cytochrome P450 in biosensors. *Bioanal Rev* 3:67–94
- Yebara DM, Kiil S, Dam-Johansen K (2004) Antifouling technology—past, present and future steps towards efficient and environmentally friendly antifouling coatings. *Prog Org Coat* 50:75–104

- Zerihun T, Gründler P (1996) Electrically heated cylindrical microelectrodes. Determination of lead on Pt by cyclic voltammetry and cathodic stripping analysis. *J Electroanal Chem* 415:85–88
- Zhang W, Li G (2004) Third-generation biosensors based on the direct electron transfer of proteins. *Anal Sci* 20:603–609
- Zoski CG (2002) Ultramicroelectrodes: design, fabrication, and characterization. *Electroanalysis* 14:1041–1051
- Zoski CG (2007) *Handbook of electrochemistry*. Elsevier Science

Amperometric and Impedance Monitoring Systems for
Biomedical Applications

Punter-Villagrasa, J.; Colomer-Farrarons, J.; del Campo,
F.J.; Miribel-Catala, P.

2017, VIII, 241 p. 145 illus., 75 illus. in color., Hardcover

ISBN: 978-3-319-64800-2